



Millimeter-Wave Photonic Techniques: Part II- All Optical Microwave Signal Processing

Jianping Yao¹, Xiupu Zhang², Raman Kashyap^{3,4} and Ke Wu⁴

¹Microwave Photonics Research Laboratory
School of Information Technology and Engineering
University of Ottawa, Ottawa, Canada

²Department of Electrical and Computer Engineering
Concordia University, Montreal, Canada

³Department of Engineering Physics
Ecole Polytechnique de Montreal, Montreal, Canada

⁴Poly-Grames Research Center, Department of Electrical Engineering
Ecole Polytechnique de Montreal, Montreal, Canada

Abstract-The distribution of broadband microwave and millimeter-wave (mm-wave) signals over optical fiber with the advantageous features such as broad bandwidth, low loss and immunity to electromagnetic interference has led to an ever-increasing interest in their use in broadband wireless access networks and broadband sensor networks. For radio over fiber (RoF) networks, it is desirable that distributed signals be processed directly in the optical domain to avoid additional optical to electrical (O/E) and electrical to optical (E/O) conversions. In this paper, three new techniques to process microwave and mm-wave signals in the optical domain, including all-optical microwave bandpass filtering and all-optical microwave mixing, are discussed.

Index Terms- radio over fiber, millimeter-wave over fiber, all-optical millimeter-wave signal processing, broadband wireless access

I. INTRODUCTION

The key function of a radio over fiber (RoF) network is to distribute microwave and millimeter-wave (mm-wave) signals over optical fiber to take the advantages of the low loss, low dispersion and large bandwidth of optical fiber links. On the other hand, it is also highly

desirable that the distributed signals can be processed directly in the optical domain without extra electrical (O/E) and electrical to optical (E/O) conversions, such as all-optical microwave filtering and mixing. A lot of efforts have been directed to the research and development of all-optical microwave mixing and filtering techniques in the last two decades. In this paper, we present some new techniques developed recently by the authors in all-optical microwave signal processing, such as all-optical microwave bandpass filtering and all-optical microwave mixing.

II. ALL-OPTICAL MICROWAVE FILTERING

The processing of microwave and mm-wave signals directly in the optical domain bring a number of advantages such as large time-bandwidth products, low loss, light weight and immunity to electromagnetic interferences. Many approaches to achieving all-optical microwave filtering have been proposed in the last two decades. The key difficulty involving in the processing of microwave signals in the optical domain is that the light source in an optical microwave filter has to be incoherent, to avoid optical interferences, which leads to the

instability of the system. The use of incoherent optical source limits the coefficients of optical delay line filters to be all positive, leading to low-pass filtering functionality only. For radio-over-fiber (RoF) applications, bandpass filtering is highly desirable. Many approaches to implementing all-optical bandpass filtering have been proposed in the past few years. One approach proposed by Sales et al. [1] is to use differential detection, which requires converting the optical signal to electrical signal at the cost of increased system complexity. Other approaches with negative coefficients for bandpass filtering include wavelength conversion based on cross-gain modulation in a semiconductor optical amplifier (SOA) [2], and carrier depletion effect in a Fabry-Perot (FP) laser diode [3] or in a distributed feedback (DFB) laser diode [4]. Recently, Capmany et al. [5] proposed a bandpass filter that employs two electro-optic modulators. Negative coefficients are obtained by biasing the two electro-optic modulators at different operation points with opposite slopes. Mora et al. [6] presented a simple approach to realizing bandpass filters with negative coefficients. The negative taps are obtained by use of the transmission of a broadband source through uniform Bragg gratings. Chan et al. [7] presented a two-tap notch filter with one negative tap, in which a dual-output electro-optic intensity modulator is used. The electro-optic intensity modulator is connected in a way that it undergoes a double-pass modulation. All these approaches are based on intensity modulation. In this Section, we present two all-optical microwave bandpass filters based on optical phase modulation, which have the features of simple configuration and easy to implement.

A. All-Optical Bandpass Microwave Filter Based on an Electro-Optic Phase Modulator

It is different from the negative coefficient bandpass filters proposed in [1-7], the bandpass filter here is realized by eliminating the baseband resonance of a typical lowpass filter using an optical phase modulator (PM) combined with a dispersive device [8, 9]. In the configuration shown in Fig. 1, an array of laser diodes emitting

at different optical wavelengths with identical wavelength spacing are phase modulated by the microwave signal to be filtered; two first-order sidebands with π phase difference are generated for each optical carrier. The phase modulated signal is then applied to a dispersive device. In the experimental setup, the dispersive device is a length of standard single mode fiber (SSMF). The filtered microwave signal is obtained at the output of a photodetector. A four-tap microwave bandpass filter is implemented. A null is always observed at dc, which ensures a bandpass operation.

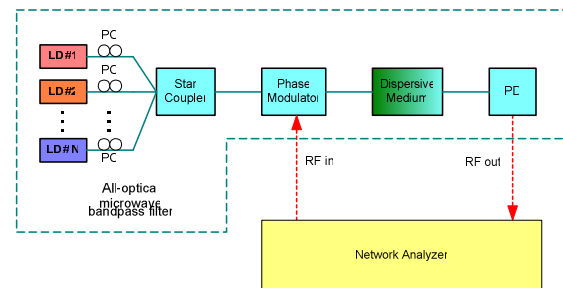


Fig. 1. Block diagram of the bandpass filter.

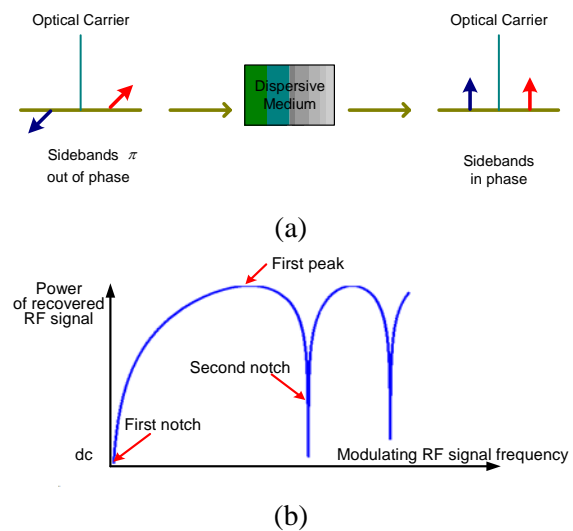


Fig. 2. Phase modulation to intensity modulation conversion. (a) Optical phase modulation. (b) Recovered RF power vs. RF frequency.

The phase modulated optical spectrum is illustrated in Fig. 2(a), which consists of an optical carrier and two first-order sidebands. In

general, the phase modulation process generates a series of sidebands with amplitude coefficients determined by Bessel functions of the first kind. However, when the modulation depth is small, the higher-order sidebands can be neglected, and only the first-order upper and lower sidebands need to be considered.

It is different from an intensity modulation where the two first-order sidebands at the output are in phase. At the output of the PM, the two first-order sidebands are π out of phase. If this signal is directly detected using a photodiode, the RF signal cannot be recovered because the beating between the carrier and the upper sideband exactly cancels the beating between the carrier and the lower sideband. However, as shown in Fig. 2(a), if the modulated optical signal passes through a dispersive device, the phase difference between the two sidebands can be effectively rotated to be totally or partially in phase thanks to the chromatic dispersion induced by the dispersive device. Then the modulating RF signal may be recovered when this dispersed optical signal is fed to a photodetector. Mathematically, the recovered microwave signal can be expressed by (1), which shows that the amplitude of the recovered RF signal, denoted as $E_{RF}(t)$, is the function of the system-induced dispersion as well as the modulating frequency,

$$E_{RF}(t) \propto \cos\left(\frac{\pi \chi \lambda_0^2 f_m^2}{c} + \frac{\pi}{2}\right) \cdot \cos(2\pi f_m t + \phi) \quad (1)$$

where c is the optical wave propagation velocity in free space; χ is the chromatic dispersion of the dispersive device; λ_0 is the central wavelength of the carrier; f_m is the frequency of the modulation signal; and ϕ is the phase delay of the recovered microwave signal, which is also determined by χ and f_m . Based on (1), the frequency response of this phase modulation and intensity-detection operation is denoted as $H_1(\omega)$ and is drawn in Fig. 2(b). We can see that there is a notch at the dc frequency; the first peak and the second notch can be calculated by letting $\pi \chi \lambda_0^2 f_m^2 / c = \pi/2$ and π , respectively.

Now an array of laser diodes are phase modulated by the phase modulator. Each laser source can be considered as an independent optical carrier. If we assume that the wavelength spacing between any adjacent laser diode is very small and all the laser diodes have identical input power at the phase modulator, the dispersion effects induced frequency response ($H_1(\omega)$) for each carrier can be considered identical. But the phase ϕ_n of the n -th RF signal recovered from the n -th modulated optical signal is not identical because different carrier travels at different velocity in this dispersive device. Then the summation of all the recovered RF signals will induce another frequency response $H_2(\omega)$, which can be expressed as

$$H_2(\omega) \propto \sum_{n=1}^N \exp(j\phi_n) = \sum_{n=1}^N \exp[j\omega_m \cdot (n-1) \cdot T] \quad (2)$$

where N is the number of the laser diodes or the number of the filter taps, ϕ_n is the phase of the n -th recovered RF signal, ω_m is the modulating angle frequency, and $T = \chi \cdot \Delta\lambda$ is the time interval of any two adjacent taps.

The effective transfer function of this PM-based microwave filter can be expressed as the multiplication of the two responses,

$$H(\omega) = H_1(\omega) \cdot H_2(\omega) \quad (3)$$

Based on the characteristics of $H_1(\omega)$ and $H_2(\omega)$ discussed earlier, we may conclude that the baseband resonance of the lowpass filtering function due to the conventional intensity-modulation direct-detection (IM-DD) scheme can be eliminated; and an all-optical equivalent bandpass microwave filter is consequently achieved.

An experiment based on the configuration shown in Fig. 2(a) is carried out. In the experimental setup, a four-tap all-optical bandpass microwave filter is implemented using 4 tunable lasers emitting at wavelengths of 1567.83, 1568.03, 1568.23 and 1568.42 nm to feed to a high-speed

electro-optic PM via a star coupler. The pumping current and polarization state of each laser source are carefully adjusted to obtain a window function of $\{0.54, 1, 1, 0.54\}$, as shown in Fig. 3(a). A coil of 25 km SSMF is used as the dispersive device. The wavelength spacing between any two adjacent laser diodes is around 0.2 nm, which gives a time delay of 90 ps or a free spectral range (FSR) of 11.1 GHz. This FSR ensures that the resonance peak of $H_2(\omega)$ is located at the same position as the first peak of $H_1(\omega)$.

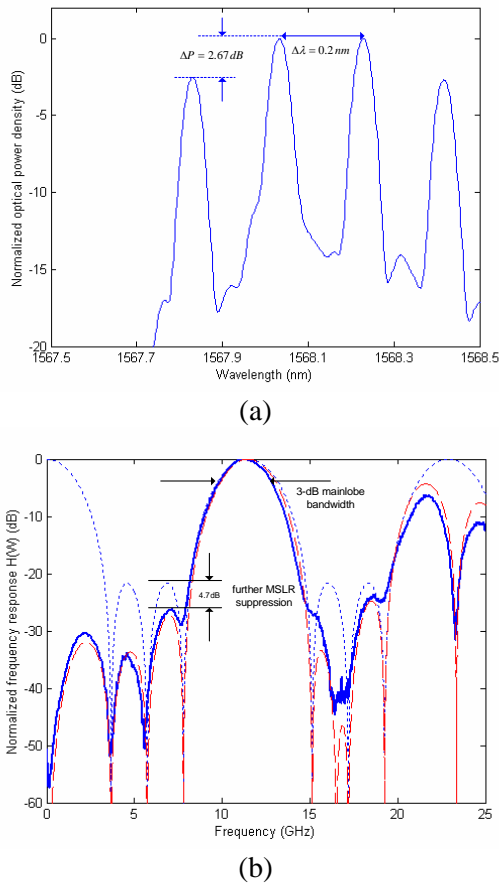


Fig. 3. Experimental results of the bandpass filter with a window function $\{0.54, 1, 1, 0.54\}$. (a) Optical spectrum of the laser array; (b) frequency responses: measured $H(\omega)$ (solid line), theoretical $H_1(\omega)$ (dashed line), theoretical $H_2(\omega)$ (dotted line).

The effective transfer function of the microwave filter $H(\omega)$, shown in Fig. 3(b), is measured

using a vector network analyzer (VNA), an excellent agreement between the theoretical and experimental results are observed.

The proposed scheme here has certain advantages compared with some earlier approaches. First, it has a simpler structure with less optical components. In the proposed structure, only an electro-optic PM, a laser array and a dispersive device are required; whereas in other approaches complicated structure and additional components are required, such as SOAs in cross-gain modulation approach, a second electro-optic modulator, or a special dual-output electro-optic modulator, are required to implement bandpass filters with negative coefficients. Another important advantage provided by this approach is that it has the potential to be reconfigurable and tunable. The output power of each laser diode in the laser array can be adjusted independently, which means that different window functions can be easily applied to the filter and therefore the frequency response can be reconfigured. Furthermore, the same dispersive device is used to synthesize both the transfer functions of $H_1(\omega)$ and $H_2(\omega)$, which implies that by adopting more taps, and carefully selecting the carrier wavelengths or the dispersive medium with proper chromatic dispersion, the synthesis of some practical and tunable bandpass filters is possible.

B. All-Optical Microwave Bandpass Filter with Negative Coefficients

It is different from the approach above, here the bandpass filter has negative coefficients that are generated through phase modulation to intensity modulation (PM-IM) conversion by an optical filter [10]. In the configuration, two laser sources are tuned to have the optical wavelengths at the quadrature frequencies of the positive and negative slopes of the transfer function of the optical filter. The optical carriers generated by the two laser sources are phase modulated by a RF signal generated from a VNA; the phase-modulated optical signals are fed into the optical filter, in which the phase-modulated signals are converted to intensity-modulated signals. The

envelopes of the converted signals will be π out of phase because their carriers are tuned at the opposite slopes of the optical transfer function of the optical filter. The converted signals from the optical filter are then applied to a length of SSMF serving as a dispersive device to provide different time delays. The filtered RF signal is recovered by a photodetector. A two-tap bandpass transversal microwave filter based on the proposed scheme is implemented.

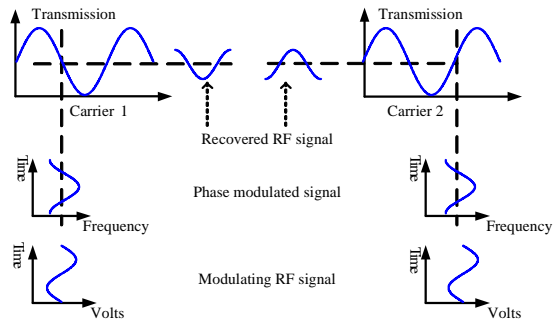


Fig. 4. Implementation of negative coefficients based on PM-IM conversion using an optical filter.

The fundamental concept for the implementation of negative coefficients is shown in Fig. 4. The optical filter can be an unbalanced Mach-Zehnder interferometer or a Sagnac loop with a typical transmission function shown at the top of the figure. Two optical carriers, namely carrier 1 and carrier 2, are tuned at the opposite slopes of the filter transfer function. The same RF modulating signal is modulated on the two carriers via a PM, which will introduce an instant frequency shift to the carriers. The value of the frequency shift is proportional to the differential of the RF modulating signal. Under this situation, the optical filter is equivalent to a frequency discriminator, by which the frequency shift is converted to the variation of optical intensity. It can be seen from Fig. 4, if the two carriers are phase modulated, the output optical signals from the optical filter will be with the same power but with the modulating signals in counter-phase, negative coefficient is thus obtained.

The experimental setup is shown in Fig. 5(a). Two tunable laser sources are used to provide the tunable carriers. The two carriers from the two

tunable laser sources are phase modulated by a RF signal generated by a VNA and then fed into a Sagnac loop serving as the optical filter. The intensity transfer function of the Sagnac loop is shown in Fig. 5(b). As can be seen that the optical filter has a free spectral range, FSR_λ , of around 0.19 nm. A time delay difference is obtained by passing the optical carriers through a 25-km SSMF, which has a dispersion of 425 ps/nm at 1550 nm.

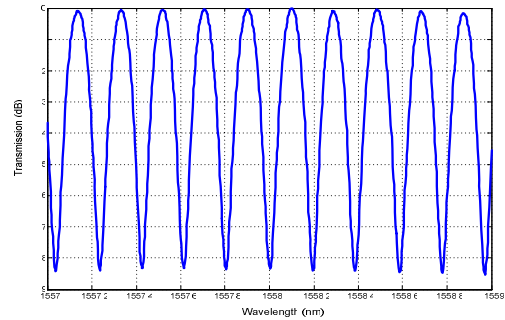
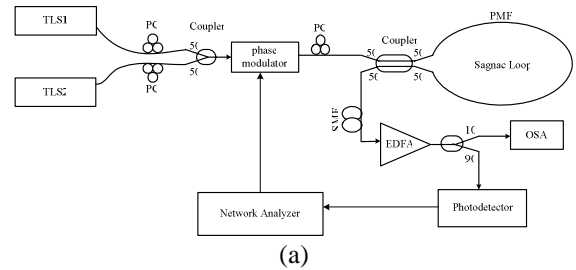


Fig. 5. (a) Block diagram of the proposed all-optical microwave bandpass filter. (b) Transfer function of the Sagnac-loop optical filter. PC: polarization controller; PMF: polarization maintaining fiber; OSA: optical spectrum analyzer.

Based on the discussion, it is expected that if the wavelength of the first tunable laser source, namely λ_1 , is fixed at the quadrature point of one positive slope, different microwave transfer functions will be achieved when the wavelength of the second tunable laser source, namely λ_2 , is tuned to satisfy the conditions $|\lambda_1 - \lambda_2| = (2n + 1)(FSR_\lambda / 2)$ or $|\lambda_1 - \lambda_2| = (2n)(FSR_\lambda / 2)$, where $n = 0, 1, 2, 3 \dots$. In the first case, a bandpass frequency response is expected since λ_1 and λ_2 are at the opposite slopes; on the other hand, a

lowpass frequency response will be obtained in the second case because λ_1 and λ_2 are at the equal slopes.

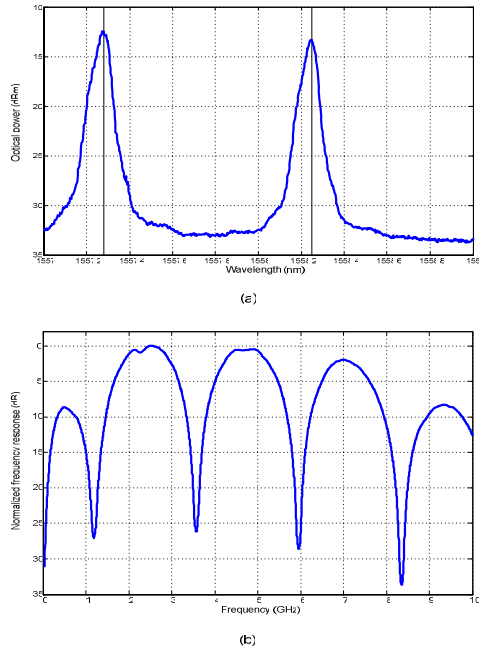


Fig. 6. Bandpass-equivalent filter with only positive coefficients. (a) Optical spectrum of the two tunable laser sources; (b) Frequency response of the bandpass-equivalent filter.

Firstly, λ_1 is fixed at 1557.282 nm, and λ_2 is tuned to 1558.246 nm, as shown in Fig. 6(a). The spacing between λ_1 and λ_2 is 0.964 nm, which is 5 times of the FSR_λ . Since the wavelengths of the two carriers are located at the points with equal slopes, no negative coefficients are obtained. As discussed earlier, the baseband resonance is suppressed by the PM-IM conversion, a bandpass-equivalent filter is obtained. The filter frequency response is shown in Fig. 6(b). As can be seen, a high sidelobe at the baseband is observed; the sidelobe is caused by the baseband resonance, which is only partially suppressed by the dc notch. The FSR of the microwave filter is 2.4 GHz, corresponding to a time delay of 410 ps.

Then λ_2 is tuned to a wavelength of 1558.336 nm, the difference between λ_1 and λ_2 is now

1.054 nm, 5.5 times of the FSR_λ , as shown in Fig. 7(a). Since the wavelengths of the two carriers are now located at the points with opposite slopes, a negative coefficient is obtained. The frequency response is shown in Fig. 7(b). It is a true bandpass filter with a negative coefficient. No sidelobe is observed at the baseband. The FSR of the filter is 2.2 GHz, which corresponds to a time delay of 448 ps.

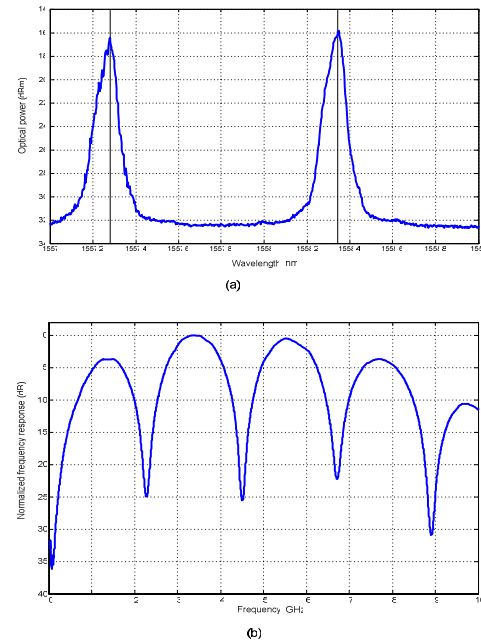


Fig. 7. True bandpass filter with a negative coefficient. (a) Optical spectrum of the two tunable laser sources. (b) Frequency response of the true bandpass filter.

The tunability of the proposed microwave filter is also investigated. When λ_2 is tuned to 1557.964 nm, the spacing between λ_1 and λ_2 is 0.682 nm, 3.5 times of the FSR_λ , as shown in Fig. 8(a). In this case, a negative coefficient is still obtained, but with a smaller time delay difference, the FSR is thus increased, as shown in Fig. 8(b). In the experiment, the FSR of the filter is 3.3 GHz, which corresponds to a time delay of 290 ps.

Note that the performance of the microwave filter, especially the notch rejection level, depends highly on the stability of the optical sources and

the optical filter. The use of state-of-the-art optical sources will solve the laser stability problem. For example, the wavelength drift of JDS-Uniphase laser diodes with case temperature is much better than $1 \text{ pm}/^\circ\text{C}$. In our experiment, the performance of the proposed microwave filter is mainly affected by the instability of the optical filter. We believe that this problem can be solved by using an optical filter with proper packaging and temperature control or by using a temperature-insensitive Sagnac loop, as reported recently in [11]. In addition, the PM-IM conversion can also be realized using a chirped FBG, as reported recently by us [12], which would increase the system stability.

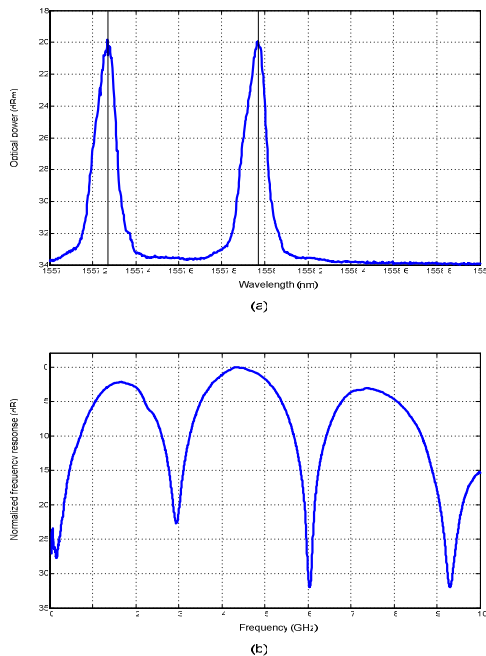


Fig. 8. Tunability of the proposed bandpass filter. (a) Optical spectrum of the two tunable lasers. (b) Frequency response of the all-optical bandpass filter.

III. ALL-OPTICAL MICROWAVE MIXING

In addition to all-optical microwave filtering, all-optical microwave mixing is another important topic in all-optical signal processing. In this Section, an approach proposed recently to achieving both all-optical mixing and all-optical filtering is discussed. The approach is based on an electro-optic phase modulator and a length of SSMF.

The first function of the PM is to perform all-optical microwave mixing. The mixed signals at the output of the PM are then fed to the SSMF link, which acts as a dispersive device for bandpass filtering, and distributes the mixed signal to a remote site. The combination of the phase modulator, a multiwavelength laser source and the SSMF link forms an all-optical microwave bandpass filter [8, 9], which can be designed to have a passband located at the up- or down-converted microwave frequency. Frequency components other than the up-converted or down-converted frequency component will be rejected.

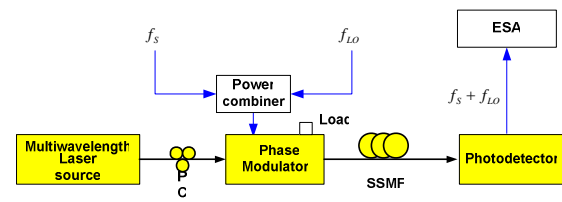


Fig. 9. Block diagram of the proposed all-optical microwave signal processor.

The block diagram of the signal processor is shown in Fig. 9. The signal processor consists of a multiwavelength laser source, an optical phase modulator and a length of SSMF. The light from the multiwavelength laser source is applied to the optical phase modulator through a polarization controller (PC). A microwave signal at frequency f_s is to be up-converted to $f_s + f_{LO}$, where f_{LO} is the frequency of the local oscillator signal. Both signals are applied to one port of the PM via a power combiner. The other port of the phase modulator is terminated in a load. The mixed optical signals after the optical PM are then applied to the SSMF link serving as a dispersive device as well as a transmission medium. The up-converted (or down-converted) electrical signal is obtained at the output of a photodetector located at the end of the fiber link.

The electrical signals applied to the optical PM have two frequencies at f_s and f_{LO} , the phase modulated optical field can be expressed in terms of Bessel functions of the first kind, which is given by

$$E(t) = \sum_{i=1}^I \sum_{n=-\infty}^{+\infty} \sum_{k=-\infty}^{+\infty} J_n[m_p(\omega_s)V_S] \cdot J_k[m_p(\omega_{LO})V_{LO}] \cdot \cos[(\omega_{c,i} + n\omega_s + k\omega_{LO})t + \frac{1}{2}n\pi + \frac{1}{2}k\pi] \quad (4)$$

where $\omega_{c,i}$ is the angular frequency of the i -th optical carrier; $m_p(\omega)$ represents the effective phase modulation index, which is a function of the microwave frequency; V_S and V_{LO} are the amplitudes of the modulating microwave signals applied to the input port of the phase modulator at frequencies of ω_s and ω_{LO} , respectively; n and k are integers representing the orders of the harmonics; and $J_n[\cdot]/J_k[\cdot]$ denotes the n -th/ k -th order Bessel function of the first kind. To simplify, the argument ($m_p(\omega)V$) will be omitted in the remainder of the paper. From (4), we can find that the phase modulated optical field consists of multiple carriers and a series of sidebands with amplitudes determined by the Bessel functions. For each carrier, the corresponding sidebands have frequency deviations from the carrier of $\pm\omega_s$, $\pm\omega_{LO}$, $\pm 2\omega_s$, $\pm 2\omega_{LO}$, ..., and $\omega_{LO} \pm \omega_s$, $2\omega_s \pm \omega_{LO}$, $2\omega_{LO} \pm \omega_s$, Meanwhile, based on the property of the Bessel function of the first kind,

$$\begin{aligned} J_n &= -J_{-n}, J_k = -J_{-k}, & \text{when } n, k \text{ are odd} \\ J_n &= J_{-n}, J_k = J_{-k}, & \text{when } n, k \text{ are even} \end{aligned} \quad (5)$$

as can be seen that the odd-order sidebands (when $|n+k|$ is odd) of each pair is π out of phase. If this phase-modulated optical signal is directly detected using a photodiode, no microwave signal but a dc can be obtained. This behavior is expected since the phase modulation does not alter the amplitude of the input optical carrier, and the square-law photodetector works like an envelope detector. However, if the phase modulated optical signal passes through a dispersive device, for example, a length of SSMF, the phase relationship between any two optical frequency components will be changed due to the chromatic dispersion of the SSMF. When this

dispersed optical signal is fed to a photodetector, microwave signals with different frequencies may be obtained, which indicates that the PM is converted to IM by the SSMF and a microwave mixing function is achieved. Furthermore, since here we use a multi-wavelength laser source and assume each lasing wavelength is independent; eventually the output RF signal at each mixing frequency is a vector summation of all the corresponding electrical signals carried by the different wavelengths with different delays. This summation may be constructive or destructive depending on the frequency of the mixing product and the dispersion of the SSMF: a transversal microwave filtering function is also achieved. The frequency response can be approximated as [11]

$$H(\omega) \propto \underbrace{\cos\left(\frac{\pi \overline{\chi}_i \overline{\lambda}_i^2 f^2}{c} + \frac{\pi}{2}\right)}_{H_1(\omega)} \cdot \underbrace{\sum_{i=1}^I P_i \cdot \exp[j2\pi f(i-1)T]}_{H_2(\omega)} \quad (6)$$

where $\overline{\chi}_i$ and $\overline{\lambda}_i$ denote the average chromatic dispersion and the mean value of the optical carrier wavelengths; P_i represents the power of the i -th optical carrier; $T = \overline{\chi}_i \cdot \Delta\lambda$ is the time interval between any two adjacent taps; $H_1(\omega)$ represents the effects of PM-IM conversion, which has a quasi-periodic frequency response with a notch at the dc frequency and the first resonance peak at $f_1 = \sqrt{c/2\overline{\chi}_i \overline{\lambda}_i^2}$ (let $H_1(\omega) = -1$); and $H_2(\omega)$ is a typical frequency response of an all-optical transversal lowpass filter, which has a periodic frequency response with the first resonance peak at the dc and the second resonance peak at $f_2 = 1/T = 1/(\overline{\chi}_i \cdot \Delta\lambda)$ (it is also the FSR of $H_2(\omega)$). The effective transfer function $H(\omega)$ of the filter is expressed as the multiplication of these two responses. By choosing proper $\overline{\chi}_i$, $\overline{\lambda}_i$, and $\Delta\lambda$ to make $f_1 = f_2$, an equivalent bandpass filter is achieved, because the baseband resonance of $H_2(\omega)$ is eliminated by the notch of $H_1(\omega)$ at dc.

Based on the above analysis, if the passband peak of the proposed microwave bandpass filter is located at the frequency of the desired mixing product, the proposed system can perform simultaneously all-optical microwave mixing and bandpass filtering. The signal processor based on the block diagram shown in Fig. 9 is built. The experiment is carried out in four steps.

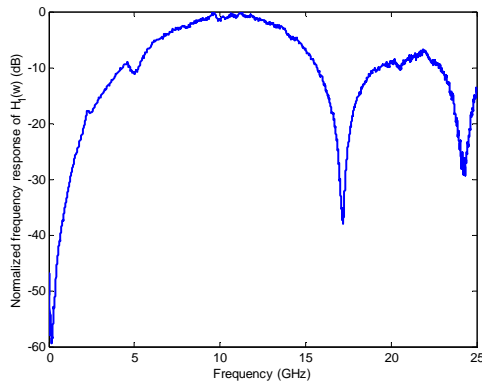


Fig. 10. Frequency response of the PM-IM conversion. A notch is observed at the DC frequency.

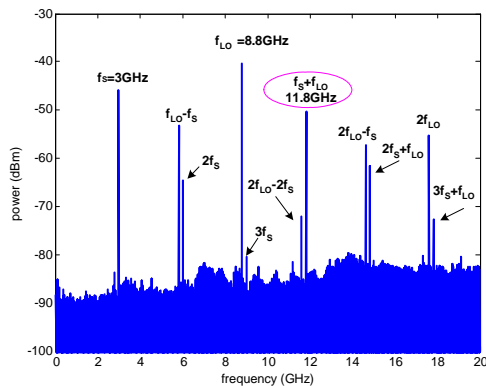


Fig. 11. Electrical spectrum of the signal at the output of the mixer, which consists of different mixing frequency components.

PM-IM conversion. Instead of using a multiwavelength laser, a single-wavelength LD with a wavelength of 1550 nm is used as the light source. A 25-km SSMF is employed as the dispersive device. The SSMF has a chromatic dispersion of 17 ps/nm/km at 1550 nm. The total chromatic dispersion of 25 km of this fiber is

$\chi = 425$ ps/nm. To experiment the PM-IM conversion, a single microwave signal is applied to the PM. By sweeping the modulating frequency from 45 MHz to 25 GHz while keeping the same output power of 3 dBm, we obtain the recovered microwave signal at the output of the photodetector. The output signal power versus the microwave frequency is shown in Fig. 10. It can be seen that the PM-IM conversion has a quasi-periodic frequency response with a notch at dc.

Microwave Mixing. Keeping the LD as the light source, instead of using a single microwave signal, we use two microwave signals operating at frequencies of $f_s = 3$ GHz and $f_{LO} = 8.8$ GHz to drive the PM. The power level for both signals is 17 dBm. The recovered microwave signals which consist of different frequency components are monitored using an electrical spectrum analyzer (ESA). As can be seen in Fig. 11, a series of microwave signals which correspond to the different frequency components of the mixing product are observed. Note that the power levels of the signals at f_s and f_{LO} are higher than the up-converted signal $f_s + f_{LO}$. Also the power levels of the higher-order harmonics ($2f_s$, $3f_s$, $2f_{LO}$, ...) and other unwanted intermodulation products ($f_{LO} - f_s$, $2f_{LO} - 2f_s$, $2f_{LO} - f_s$, $2f_s + f_{LO}$, $3f_s + f_{LO}$, ...) are comparable to that of the $f_s + f_{LO}$ component. Therefore, a bandpass filter with narrow passband and high mainlobe to sidelobe ratio must be used to suppress the unwanted frequency components.

All-optical microwave bandpass filtering. To achieve microwave filtering with very narrow bandwidth, the number of taps must be large. Many taps can be realized by using an array of LDs, but with a complicated and costly system. To simplify the signal processor, in the experiment instead of using an array of LDs, we use a multiwavelength fiber ring laser with about 30 wavelengths and a wavelength spacing of 0.2 nm proposed recently by us [22, 23]. The power spectrum of the multiwavelength laser is shown

in Fig. 12. Using this multiwavelength laser as the light source and sweeping the modulating frequency from 45 MHz to 25 GHz, we obtain the frequency response of the proposed signal processor, as shown in Fig. 13. It can be seen that the baseband resonance of the conventional intensity modulation- direct detection based all-optical microwave lowpass filter is eliminated. A bandpass filter with a 3-dB mainlobe bandwidth of 330 MHz and a mainlobe to sidelobe ratio of 30 dB is achieved. The RF frequency at the peak of the passband is of 11.8 GHz and is determined by the wavelength spacing of the multiwavelength light source and the total chromatic dispersion of the 25-km SSMF link.

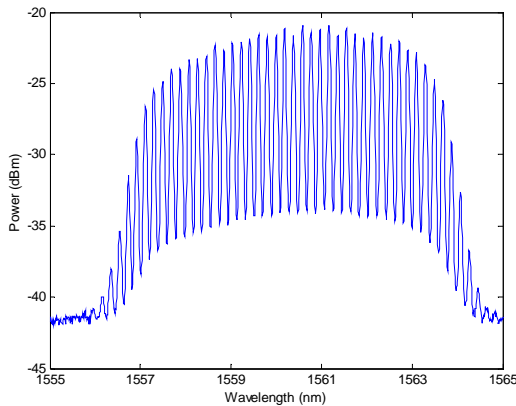


Fig. 12. Output power spectrum of the multi-wavelength fiber laser.

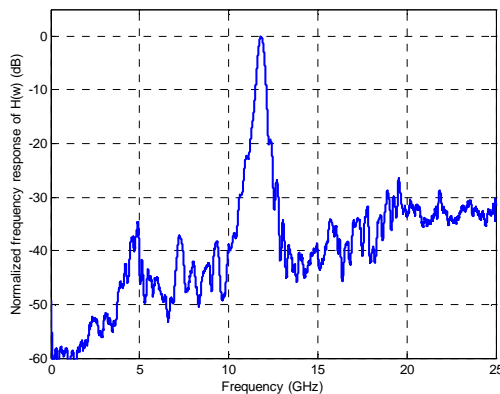


Fig. 13. Frequency response of the bandpass filter.

All-optical microwave mixing and bandpass filtering. Using the multiwavelength fiber ring laser as the light source, and applying the two signals ($f_s = 3$ GHz and $f_{LO} = 8.8$ GHz) to the

PM, we obtain an up-converted microwave signal at the output of the photodetector. As can be seen from Fig. 13, only the up-converted component at $f_s + f_{LO}$ is obtained while other frequency components are efficiently suppressed. The zoom-in spectrum with a span of 30 kHz at $f_s + f_{LO}$ is also shown as an insert in Fig. 14, which exhibits a high quality up-converted signal. Compared with the results shown in Fig. 11, a good rejection (better than 40 dB) of the unwanted frequency components is achieved. We should also note that thanks to the use of the SSMF link as the dispersive device, the up-converted signal can be naturally distributed to a remote site over a 25 km span, which provides an added advantage to the proposed system. If further dispersion management is applied, the microwave distribution distance will be flexible.

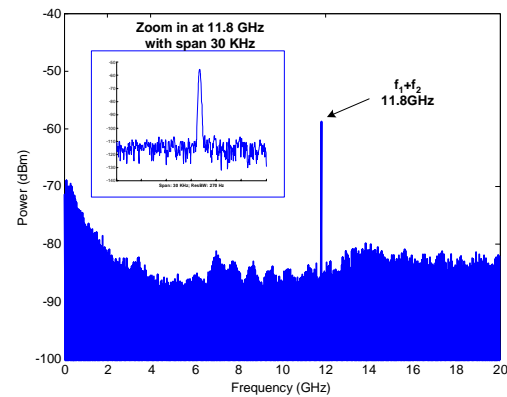


Fig. 14. Power spectrum at the output of the photodetector. Only the up-converted signal at 11.8 GHz is obtained and other frequency components are rejected.

IV. CONCLUSION

All-optical microwave signal processing has been a topic of interest for over twenty years thanks to its potential for processing broadband and high-frequency microwave signals in the optical domain, which have been difficult to implement using state-of-the-art digital signal processing (DSP) techniques due to limited electrical sampling speed. In this paper, three new approaches to implementing all-optical microwave signal processing were discussed. The

key feature of these approaches is that a phase modulator instead of an intensity modulator is used, which provides interesting properties for all-optical bandpass filtering and mixing.

ACKNOWLEDGMENT

The work is supported by the Natural Sciences and Engineering Research Council of Canada and the Canada Research Chairs Program (Wu & Kashyap).

The authors would like to acknowledge the contributions of Fei Zeng and Jun Wang of the University of Ottawa.

REFERENCES

- [1] S. Sales, J. Capmany, J. Marti, and D. Pastor, "Experimental demonstration of fiber-optic delay line filters with negative coefficients," *Electron. Lett.*, vol. 31, no. 13, pp. 1095-1096, Jun. 1995.
- [2] F. Coppinger, S. Yegnanarayanan, P. D. Trinh, and B. Jalali, "All-optical RF filter using amplitude inversion in a semiconductor optical amplifier," *IEEE Trans. Microwave Theory Tech.*, vol. 45, no. 8, pp. 1473-1477, Aug. 1997.
- [3] X. Wang and K. T. Chan, "Tunable all-optical incoherent bipolar delay-line filter using injection-locked Fabry-Perot laser and fiber Bragg gratings," *Electron. Lett.*, vol. 36, no. 24, pp. 2001-2002, Nov. 2000.
- [4] S. Li, K. S. Chiang, W. A. Gambling, Y. Liu, L. Zhang, and I. Bennion, "A novel tunable all-optical incoherent negative-tap fiber-optic transversal filter based on a DFB laser diode and fiber Bragg gratings," *IEEE Photon. Technol. Lett.*, vol. 12, pp. 1207-1209, 2000.
- [5] J. Capmany, D. Pastor, A. Martinez, B. Ortega, and S. Sales, "Microwave photonics filters with negative coefficients based on phase inversion in an electro-optic modulator," *Opt. Lett.* vol. 28, pp. 1415-1417, 2003.
- [6] J. Mora, M. V. Andres, J. L. Cruz, B. Ortega, J. Capmany, D. Pastor, and S. Sales, "Tunable all-optical negative multitap microwave filters based on uniform fiber Bragg gratings," *Opt. Lett.*, vol. 28, pp. 1308-1310, 2003.
- [7] E. H. W. Chan and R. A. Minasian, "Novel all-optical RF notch filters with Equivalent Negative Tap Response," *IEEE Photon. Technol. Lett.*, vol. 16, pp. 1370-1372, 2004.
- [8] F. Zeng and J. P. Yao, "All-optical bandpass microwave filter based on an electro-optic phase modulator," *Opt. Express*, vol. 12, no. 16, pp. 3814-3819, Aug. 2004.
- [9] F. Zeng and J. P. Yao, "Investigation of phase modulator based all-optical bandpass filter," *J. Lightwave Technol.*, vol. 23, no. 4, pp. 1721-1728, Apr. 2005.
- [10] J. Wang, F. Zeng, and J. P. Yao, "All-optical microwave bandpass filters with negative coefficients based on PM-IM conversion," *IEEE Photon. Technol. Lett.*, vol. 17, no.10, pp. 2176-21780, Oct. 2005.
- [11] D. H. Kim and J. U. Kang, "Sagnac loop interferometer based on polarization maintaining photonic crystal fiber with reduced temperature sensitivity," *Opt. Express*, vol. 12, no. 19, pp. 4490-4495, Sep. 2004.
- [12] F. Zeng, J. Wang, and J. P. Yao, "All-optical microwave bandpass filter with negative coefficients based on an electro-optic phase modulator and linearly chirped fiber Bragg gratings," *Opt.Lett.*, vol. 30, no. 17, pp. 2203-2205, Sep. 2005.
- [13] G. K. Gopalakrishnan, W. K. Burns, and C. H. Bulmer, "Microwave-optical mixing in LiNbO₃ modulators," *IEEE Trans. Microwave Theory Tech.*, vol. 41, no. 12, pp. 2383-2391, Dec. 1993.
- [14] J. L. Corral, J. Marti, and J. M. Fuster, "General expressions for IM/DD dispersive analog optical links with external modulation or optical up-conversion in a Mach-Zehnder electro-optical modulator," *IEEE Trans. Microwave Theory Tech.*, vol. 49, no. 10, pp. 1968-1976, Oct. 2001.
- [15] G. Maury, A. Hilt, T. Berceci, B. Cabon, and A. Vilcot, "Microwave-frequency conversion methods by optical interferometer and photodiode," *IEEE Trans. Microwave Theory Tech.*, vol. 45, no. 8, pp. 1481-1485, Aug. 1997.
- [16] J. Marti, F. Ramos, V. Polo, J. M. Fuster, and J. L. Corral, "Millimeter-wave generation and harmonic upconversion through PM-IM conversion in chirped fibre gratings," *Electron. Lett.*, vol. 35, no. 15, pp. 1265-1266, Jul. 1999.
- [17] K. P. Jackson, S. A. Newton, B. Moslehi, M. Tur, C. C. Cutler, J. W. Goodman, and H. J. Shaw, "Optical fiber delay line signal processing," *IEEE Trans. Microwave Theory Tech.*, vol. 33, pp. 193-209, Mar. 1985.
- [18] D. B. Hunter, R. Minasian, and P. A. Krug, "Tunable optical transversal filter based on chirped gratings," *Electron. Lett.*, vol. 31, no. 25, pp. 2207-2210, Dec. 1995.
- [19] G. Yu, W. Zhang, and J. A. R. Williams, "High-performance microwave transversal filter using fiber Bragg grating arrays," *IEEE Photon. Technol. Lett.*, vol. 12, no. 9, pp. 1183-1185, Sep. 2000.
- [20] J. Capmany, D. Pastor, A. Martinez, B. Ortega, and S. Sales, "Microwave photonics filters with negative coefficients based on phase inversion in an electro-optic modulator," *Opt. Lett.*, vol. 28, pp. 1415-1417, Aug. 2003.
- [21] E. H. W. Chan and R. A. Minasian, "Novel all-optical RF notch filters with Equivalent Negative

- Tap Response," *IEEE Photon. Technol. Lett.*, vol. 16, no. 5, pp. 1370-1372, May 2004.
- [22] J. Yao, J. P. Yao, Z. Deng, and J. Liu, "Multiwavelength erbium-doped fiber ring laser incorporating an SOA-based phase modulator," *IEEE Photon. Technol. Lett.*, vol. 17, no. 4, pp. 756-758, Apr. 2005.
- J. Yao, J. P. Yao, Z. Deng, and J. Liu, "Investigation of a multiwavelength fiber ring laser that incorporates a semiconductor optical amplifier as a phase modulator," *J. Lightwave Technol.*, vol. 23, no. 8, pp. 2484-2490, Aug. 2005.